Proc. of the 3rd International Conference on Electrical, Communication and Computer Engineering (ICECCE)
12-13 June 2021, Kuala Lumpur, Malaysia

Improving the Performance of MIMO Mobile-to-Mobile Fading Channel Simulators Using New Parameterization Methods

Omar Alzoubi
Department of Communication Engineering
Al-Wataniya Private University
Hama, Syria
Omar.Zouabi@wpu.edu.sy

***Abstract*— Mobile-to-mobile (M2M) communications is considered one of the new technologies to improve the spectral efficiency in mobile communication systems. In this paper, a two-ring model is used for modelling multiple-input multiple-output (MIMO) M2M channels. The modelling and simulation of MIMO fading channels is studied for both isotropic- and non-isotropic scattering cases for two-ring model, so in this context, three methods for MIMO simulation channel models are studied: Extended Method of Exact Doppler Spread (EMEDS), Modified Method of Equal Areas (MMEA) and Method Lp-Norm (LPNM). Three new methods are also suggested to design the simulation model of MIMO channel: Modified Extended Method of Exact Doppler Spread (MEMEDS), New Modified Method of Equal Areas (NMMEA) and Modified Lp-Norm method (MLPNM). The performance of each proposed method is compared with the original method by comparing the statistical properties of the reference and simulation models.**

Keywords*— Modified Extended Method of Exact Doppler Spread, New Modified Method of Equal Areas, Modified Lp- Norm Method

I. INTRODUCTION

Mobile-to-mobile (M2M) communications play a great role in many applications, such as ad-hoc wireless networks [1], intelligent transportation systems [2], and relay-based cellular networks [3]. The popularity of M2M communications has increased in the 5G cellular networks, as it enables enormous wireless machines to communicate without human interference [4]. In M2M systems both the transmitter (Tx) and the receiver (Rx) are in motion and equipped with low elevation antennas, which result in statistical properties that are completely different from those of conventional fixed-to-mobile (F2M) cellular radio systems [5]. For the development of M2M communication systems, the knowledge of the underlying propagation channel is required. For the development of M2M channel models, the regular-shaped geometry-based stochastic model (RS-GBSM) is widely used, which assumes that the effective scatterers are static and located in a regular geometric shape, such as the one-ring, two-ring, or ellipse model that is usually presented in the two-dimensional (2-D) domain. In [6], new methods were suggested to design the simulation model of multiple-input multiple-output (MIMO) Rayleigh fading channels for both isotropic- and non-isotropic scattering cases. In [5],[7], a 2-D two-ring RS-GBSM for isotropic single-input single-output (SISO) M2M Rayleigh fading channels was proposed, while [8] presents a 2-D two-ring RS-GBSM considering only double-bounce components for MIMO M2M Rayleigh fading channels in outdoor macro-cells. In [9], the 2-D two-ring RS-GBSM proposed in [8] was generalized to non-isotropic MIMO M2M Ricean fading channels in both outdoor macro- and microcells. This model takes into account the line-of-sight (LOS) component, as well as single-bounce, and double-bounce components. In addition, narrowband and wideband 2-D RS-GBSMs were proposed in [10] and [11], respectively, for non-isotropic MIMO M2M Ricean fading channels. The existing M2M channel models were classified and future challenges were identified in [12].

In this paper, we study the following three methods used for modelling the MIMO M2M channels: EMEDS, MMEA and LPNM. Three new methods are also suggested to design the simulation model of MIMO channel: MEMEDS, NMMEA and MLPNM. The performance of each proposed method is compared with the original method by comparing the statistical properties of the reference and simulation models. In Section I and section II, the theoretical- and simulation two-ring models for M2M channels are described. Computation methods for simulation model parameters are presented in Section III. The performance evaluation of the two-ring simulation model for isotropic- and non-isotropic scattering cases is investigated in Section IV. Finally, a summary of the main points of this paper is shown in section V.

II. THEORETICAL TWO-RING MODEL FOR M2M CHANNELS

This paper considers a two-ring model proposed in [8] and shown in Fig. 1, which is used for modelling MIMO M2M

978-1-6654-3897-1/21/$31.00 ©2021 IEEE

Rayleigh fading channels in outdoor macro-cells. In this model, the transmitter is the Base Station (BS) and the receiver is the Mobile Station (MS). Only scatterers located in two rings around the Tx and Rx, are taken into account. The geometrical two-ring model is suitable for environments in which both the Tx and Rx are surrounded by a large number of scatterers, such as cities and suburban areas. The double-bounce components are taken into consideration in this model, whereas LOS component between the Tx and Rx is neglected, and around the Tx and Rx, M and N scatterers lie on the ring, respectively. The symbols S_m^T and S_n^R denote the mth and nth scatterer around the Tx and Rx, respectively. The other parameters in Fig. 1 are defined in Table 1.

TABLE 1: PARAMETERS OF TWO-RING CHANNEL MODEL IN FIG. 1.

Parameters	Definitions
D	Distance between the Tx and Rx
R_T, R_R	Radii of the two rings at the Tx and Rx
δ_T, δ_R	Spacing between two adjacent antenna elements at the Tx and Rx
β_T, β_R	Orientations of the Tx and Rx antenna array relative to the x-axis
v_T, v_R	Speeds of the Tx and Rx mobile stations
α_v^T, α_v^R	Moving directions of the Tx and Rx in the x − y plane
α_m^T $(m = 1,2,...,M)$	AOD of the waves that impinges on the mth scatterer S_m^T
α_n^R $(n = 1,2,...,N)$	AOA of the wave scattered from S_n^R
D_{1m}^T, D_{2m}^T	Distances: $A_1^T - S_m^T$ and $A_2^T - S_m^T$
D_{n1}^R, D_{n2}^R	Distances: $A_1^R - S_n^R$ and $A_2^R - S_n^R$
D_{mn}^{TR}	Distance: $S_m^T - S_n^R$

The reference model of the two-ring channel assumes that the number of local scatterers around the Tx and Rx are infinite. For simplicity, the reference model of the 2×2 M2M channel is studied. The received complex channel gain $h_{11}(t)$ of the M2M communication link from A_1^T to A_1^R can be written as follows [8]:

$$h_{11}(t) = \lim_{\substack{M\to\infty \\ N\to\infty}} \frac{1}{\sqrt{MN}} \sum_{m=1}^{M}\sum_{n=1}^{N} a_m b_n c_{mn} e^{j[2\pi(f_m^T + f_n^R)t + \theta_{mn}]} \quad (1)$$

where:

$$a_m = e^{j\pi\frac{\delta_T}{\lambda}\cos(\alpha_m^T - \beta_T)} \quad (2)$$

$$b_n = e^{j\pi\frac{\delta_R}{\lambda}\cos(\alpha_n^R - \beta_R)} \quad (3)$$

$$c_{mn} = e^{j\frac{2\pi}{\lambda}\left[R_T\cos(\alpha_m^T) - R_R\cos(\alpha_n^R)\right]} \quad (4)$$

$$f_m^T = f_{\max}^T \cos(\alpha_m^T - \alpha_v^T) \quad (5)$$

$$f_n^R = f_{\max}^R \cos(\alpha_n^R - \alpha_v^R) \quad (6)$$

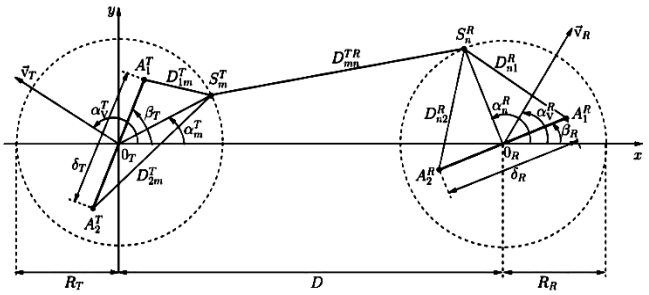

Fig. 1. Two-ring channel model [8]

The symbols λ, $f_{\max}^T$ and $f_{\max}^R$ indicate the wavelength and the maximum Doppler frequency at the Tx and Rx, respectively, and the phases θ_{mn} are random variables uniformly distributed within the interval $[0, 2\pi]$. The complex channel gain $h_{22}(t)$ of the link from A_2^T to A_2^R is obtained from (1) by making the two substitutions $a_m^* \leftarrow a_m, b_n^* \leftarrow b_n$. Similarly, we obtain $h_{12}(t), h_{21}(t)$ by replacing a_m with a_m^* and b_n with b_n^*, respectively. The complex channel matrix for the links from A_q^T to A_p^R is given by:

$$H(t) = \left[h_{pq}(t)\right] = \begin{pmatrix} h_{11}(t) & h_{12}(t) \\ h_{21}(t) & h_{22}(t) \end{pmatrix} \quad (7)$$

As the number of local scatterers around the Tx and Rx are infinite in the reference channel model, the discrete AOAs α_R^n and AODs α_T^m can be replaced by continuous quantities α_R and α_T, respectively. Without loss of generality, the von Mises PDF [13] is used to describe the distribution of the AOA and AOD according to:

$$f(\alpha) = \frac{\exp[\kappa\cos(\alpha - \mu)]}{2\pi I_0(\kappa)} \quad (8)$$

where $\alpha \in [-\pi, \pi)$, $I_0(\cdot)$ is the zeroth-order modified Bessel function of the first kind, $\mu \in [-\pi, \pi)$ is the mean angle, and κ $(\kappa \geq 0)$ controls the angular spread of the scatterers around the mean angle μ. For $\kappa = 0$ (isotropic scattering), the von Mises probability density function (PDF) reduces to the uniform distribution, while for $\kappa > 0$ (non-isotropic scattering), the von Mises PDF approximates different distributions depending on the chosen value of κ [13]. If we apply the von Mises PDF to the AOD α_T and AOA α_R, we obtain the following expressions:

$$f(\alpha_T) = \frac{\exp[\kappa_T\cos(\alpha_T - \mu_T)]}{2\pi I_0(\kappa_T)} \quad (9)$$

$$f(\alpha_R) = \frac{\exp[\kappa_R\cos(\alpha_R - \mu_R)]}{2\pi I_0(\kappa_R)} \quad (10)$$

The correlation functions (CFs) of the Tx and Rx in the M2M

MIMO system are given by [8]:

$$\rho_T(\delta_T,\tau)=\int_{-\pi}^{\pi} e^{j2\pi\frac{\delta_T}{\lambda}\cos(\alpha^T-\beta_T)-j2\pi f_{\max}^T\cos(\alpha^T-\alpha_v^T)\tau} f(\alpha^T)d\alpha^T \quad (11)$$

$$\rho_R(\delta_R,\tau)=\int_{-\pi}^{\pi} e^{j2\pi\frac{\delta_R}{\lambda}\cos(\alpha^R-\beta_R)-j2\pi f_{\max}^R\cos(\alpha^R-\alpha_v^R)\tau} f(\alpha^R)d\alpha^R \quad (12)$$

Using (9) and (10) and substituting $\delta_T=\delta_R=0$ in (11) and (12), we obtain the auto correlation function (ACF) of the complex channel gain as follows [8]:

$$r_{h_{pq}}(\tau)=\rho_T(0,\tau)\cdot\rho_R(0,\tau) \quad (13)$$

II. Simulation Two-Ring Model for M2M Channels

The simulation model of the two-ring channel assumes a finite number of local scatterers around the Tx and Rx, thus the channel matrix $\tilde{H}(t)=[\tilde{h}_{pq}(t)]$ becomes a deterministic and temporal dependent. The received complex channel gain $\tilde{h}_{11}(t)$ of the M2M communication link from A_1^T to A_1^R can be written as follows [14]:

$$\tilde{h}_{11}(t)=\frac{1}{\sqrt{MN}}\sum_{m=1}^{M}\sum_{n=1}^{N}a_m b_n c_{mn}e^{j\{2\pi[f_m^T(\alpha_m^T)+f_n^R(\alpha_n^R)]t+\theta_{mn}\}} \quad (14)$$

where the parameters a_m, b_n, c_{mn} and $f_n^R(\cdot), f_m^T(\cdot)$ are given by (2)-(6), respectively. However, since all the parameters of the deterministic simulation model are constant, the channel matrix $\tilde{H}(t)=[\tilde{h}_{pq}(t)]$ is defined for all time values. The three-dimensional cross correlation function (3D-CCF) of the simulation model for MIMO tow-ring channel is given by [14]:

$$\tilde{\rho}_{11,22}(\delta_T,\delta_R,\tau)=\frac{1}{MN}\sum_{m=1}^{M}\sum_{n=1}^{N}a_m^2(\delta_T)b_n^2(\delta_R)e^{-j2\pi(f_m^T+f_n^R)\tau} \quad (15)$$

The correlation functions (CFs) of the Tx and Rx are given by [14]:

$$\tilde{\rho}_T(\delta_T,\tau)=\frac{1}{M}\sum_{m=1}^{M}a_m^2(\delta_T)e^{-j2\pi f_m^T\tau} \quad (16)$$

$$\tilde{\rho}_R(\delta_R,\tau)=\frac{1}{N}\sum_{n=1}^{N}b_n^2(\delta_R)e^{-j2\pi f_n^R\tau} \quad (17)$$

The ACF of the complex channel gain for the simulation model is given by [8]:

$$\tilde{r}_{h_{pq}}(\tau)=\frac{1}{MN}\sum_{m=1}^{M}\sum_{n=1}^{N}e^{-j2\pi(f_m^T+f_n^R)\tau} \quad (18)$$

III. Computation Methods For Simulation Model Parameters

In order to design the simulation model of the MIMO channel, certain methods are used to find appropriate values for model parameters, so that the statistical properties of the simulation model are close enough to those of the reference model, so in this context, three methods for computing the parameters of the MIMO simulation channel models are studied: EMEDS, MMEA and LPNM. Three new methods are also suggested to design the simulation model of MIMO channel: MEMEDS, NMMEA and MLPNM.

A. Extended Method of Exact Doppler Spread (EMEDS)

The EMEDS was introduced in [14] as an extension of the Method of Exact Doppler Spread (MEDS) presented in [15], where the latter is used to calculate the parameters of channel models based on the Sum-Of-Sinusoids (SOS) principle. The EMEDS is applied in MIMO channel modelling of symmetrical Power Spectral Density (PSD), that is, isotropic scattering around the Tx and Rx, where the scatterers are positioned and uniformly distributed over two rings centered on the Tx and Rx. The parameters of the simulation model AODs α_m^T and AOAs α_n^R according to this method are given by:

$$\alpha_m^T=\frac{2\pi}{M}(m-\frac{1}{2})+\alpha_v^T, m=1,2,..,M \quad (19)$$

$$\alpha_n^R=\frac{2\pi}{N}(n-\frac{1}{2})+\alpha_v^R, n=1,2,..,N \quad (20)$$

B. Modified Method of Equal Areas (MMEA)

There are several methods used to find the parameters of the channel models based on the principle of Sum-Of-Cisoids (SOC) in the case of non-isotropic scattering [3], where the MMEA gives a good solution for such cases. The MMEA [16,17] is a modified version of the Method of Equal Areas (MEA) presented in [18]. The MEDS + MEA is proposed in [19] that combines the two properties of MEDS and MEA. The MMEA is used to design channel simulation models for non-isotropic scattering, and it can also be applied for any given distribution of AODs α_m^T and AOAs α_n^R. The parameters of the simulation model according to this method are given by:

$$\frac{m-1/4}{M}-\int_{\mu_T-\pi}^{\alpha_m^T} f(\alpha^T)d\alpha^T=0, m=1,2,..,M \quad (21\text{-a})$$

$$\frac{n-1/4}{N}-\int_{\mu_R-\pi}^{\alpha_n^R} f(\alpha^R)d\alpha^R=0, n=1,2,..,N \quad (21\text{-b})$$

where μ_T and μ_R are the means of the distributions $f(\alpha^T)$ and $f(\alpha^R)$ for AODs α_m^T and AOAs α_n^R, respectively. The parameters α_m^T and α_n^R are calculated numerically by finding the roots of equations (21-a) and (21-b).

C. Lp-Norm Method (LPNM)

The LPNM is used in the case of non-isotropic scattering around the Tx and Rx. The parameters α_m^T and α_n^R are found by minimizing the following two Lp-error norms [3]:

$$E_T^{(p)}=\left\{\frac{1}{\delta_{\max}^T\tau_{\max}^T}\int_0^{\delta_{\max}^T}\int_0^{\tau_{\max}^T}\left|\rho_T(\delta_T,\tau)-\tilde{\rho}_T(\delta_T,\tau)\right|^p d\delta_T d\tau\right\}^{1/p} \quad (22)$$

$$E_R^{(p)}=\left\{\frac{1}{\delta_{\max}^R\tau_{\max}^R}\int_0^{\delta_{\max}^R}\int_0^{\tau_{\max}^R}\left|\rho_R(\delta_R,\tau)-\tilde{\rho}_R(\delta_R,\tau)\right|^p d\delta_R d\tau\right\}^{1/p} \quad (23)$$

where $p = 1, 2, \ldots$, the parameters $\tau_{\max}^{T}, \tau_{\max}^{R}, \delta_{\max}^{T}, \delta_{\max}^{R}$ determine the maximum range within the approximations $\rho_T(\delta_T, \tau) \approx \tilde{\rho}_T(\delta_T, \tau)$ and $\rho_R(\delta_R, \tau) \approx \tilde{\rho}_R(\delta_R, \tau)$ are to be achieved. The principle of this method is based on optimizing the parameters α_m^T and α_n^R from starting values of the model parameters using the MMEA.

D. Modified Extended Method of Exact Doppler Spread (MEMEDS)

This proposed method is used to find the parameters of the simulation model AODs α_m^T and AOAs α_n^R in the case of isotropic scattering around the Tx and Rx. The parameters of the simulation model according to this method are given by:

$$\alpha_m^T = \frac{2\pi}{M} m + \alpha_v^T, m = 1, 2, \ldots, M \tag{24}$$

$$\alpha_n^R = \frac{2\pi}{N} n + \alpha_v^R, n = 1, 2, \ldots, N \tag{25}$$

where α_v^T and α_v^R are the angles of rotation with respect to the Tx and Rx and are given by:

$$\alpha_v^T = \frac{\alpha_m^T - \alpha_{m-1}^T}{2} = \frac{\pi}{M} \tag{26}$$

$$\alpha_v^R = \frac{\alpha_n^R - \alpha_{n-1}^R}{2} = \frac{\pi}{N} \tag{27}$$

E. New Modified Method of Equal Areas (NMMEA)

The proposed method is useful for finding the parameters of the MIMO channel simulation model in the case of non-isotropic scattering around the Tx and Rx. Some modifications were made to the MMEA, so that the absolute error of the simulation model's transmitter CF is minimal. The absolute error function is given by:

$$e_T(\delta_T, \tau) = \left| \rho_T(\delta_T, \tau) - \tilde{\rho}_T(\delta_T, \tau) \right| \tag{28}$$

According to the proposed method, the AODs α_m^T and AOAs α_n^R have to be determined by finding the roots of the following sets of equations:

$$\begin{aligned} \frac{m - 0.55}{M} - \int_{\mu_T - \pi}^{\alpha_m^T} f(\alpha^T) d\alpha^T = 0, m = 1, 2, .., M \\ \frac{n - 0.55}{N} - \int_{\mu_R - \pi}^{\alpha_n^R} f(\alpha^R) d\alpha^R = 0, n = 1, 2, .., N \end{aligned} \tag{29}$$

F. Modified Lp-Norm Method (MLPNM)

The proposed method can be applied to design the simulation model in the case of non-isotropic scattering around the Tx and Rx. According to MLPNM, the parameters α_m^T and α_n^R are found by minimizing the two Lp-error norms which are given in (22) and (23). This proposed method is based on optimizing the parameters α_m^T and α_n^R from starting values of the model parameters using the NMMEA.

IV. Performance Evaluation of the Tow-Ring Simulation Model

The performance of the simulation model can be evaluated by comparing its statistical properties with those of the reference model, therefore to achieve this purpose, we will evaluate the performance of different parameter computation methods by comparing ACFs, CFs of both reference and simulation models. The EMEDS and MEMEDS can be used to design the two-ring simulation model in the case of isotropic scattering, whereas the MMEA, NMMEA, LPNM and MLPNM can be applied in the case of non-isotropic scattering.

1) Isotropic Scattering case

Here, we will apply EMEDS and MEMEDS to design the simulation model in the case of isotropic scattering. The number of scatterers must be within the range $[40, 50]$ [3]. Our goal is to find the two sets $\{\alpha_m^T\}_{m=1}^{M}$ and $\{\alpha_n^R\}_{n=1}^{N}$, such that the CFs of the Tx and Rx of the simulation model are close enough to the CFs corresponding to the reference model. The parameters of the reference model AODs α^T and AOAs α^R in the case of isotropic scattering are uniformly distributed i.e. $\kappa_T = \kappa_R = 0$, and $f(\alpha^T) = f(\alpha^R) = \frac{1}{2\pi}$. We choose the following parameters of the two-ring reference model: $\alpha_v^T = 60^\circ, \beta_T = 90^\circ, f_{\max}^T = 91[Hz]$. Fig. 2 shows ACFs comparison of the reference and simulation models using EMEDS and MEMEDS for the number of scatterers around the Tx $M = 45$. We observe that the approximation $r_{h_{pq}}(\tau) \approx \tilde{r}_{h_{pq}}(\tau)$ is excellent over the range $[0, M/4]$, therefore, by increasing the number of scatterers around the Tx, we obtain a better fit between the reference and simulation models for ACFs in the case of isotropic scattering.

The behavior of the transmitter CFs for the reference and simulation models using the EMEDS and MEMEDS is studied in Fig. 3 and Fig. 4. The absolute error function which is given in (28), was also drawn in Fig. 3 and Fig. 4 in order to compare the performance of the EMEDS and MEMED. It was observed that the EMEDS and MEMEDS give the same performance for CFs at the transmitter, because both methods give an absolute error value close to zero for the number of scatterers $M = 45$ as shown in Fig. 3 and Fig. 4.

2) Non-isotropic Scattering case

In the case of non-isotropic scattering, the MMEA, NMMEA, LPNM and MLPNM are used to design the two-ring simulation model, and the AOD α_T and AOA α_R have a Von Mises distribution in the reference model, therefore, we choose $\kappa_T = 30, \mu_T = 60^\circ$ in this case. For the parameters of the reference model, we set the same values. Fig. 5 shows ACFs comparison of the reference and simulation models using the MMEA and NMMEA for the number of scatterers around the Tx $M = 45$. We observe that the approximation

$r_{h_{pq}}(\tau) \approx \tilde{r}_{h_{pq}}(\tau)$ is excellent over the range $\left[0, M/16\right]$, therefore, by increasing the number of scatterers around the Tx, we obtain a better fit between the reference and simulation models for ACFs in the case of non-isotropic scattering.

The behavior of the transmitter CFs for the reference and simulation models using the MMEA and NMMEA is studied in Fig. 6 and Fig. 7. It was observed that the error function has a ripple behavior and takes a maximum value $\max\{e_T(\delta_T,\tau)\} = 0.03$ for the MMEA, whereas the maximum error value is $\max\{e_T(\delta_T,\tau)\} = 0.02$ for the NMMEA, thus the NMMEA is superior to the MMEA by obtaining a two-ring simulation with a spatial characteristics very close to those of the reference model, whereas both methods give the same performance in terms of temporal correlation properties.

Fig. 8 shows the ACFs for the reference and simulation models using the LPNM and MLPNM. It was noticed that the ACFs of the reference and simulated models converge to each other within the range $\left[0, M/25\right]$, therefore, by increasing the number of scatterers around the Tx, we get a better fit between the reference and simulation models for ACFs. So we can say that both the LPNM and MLPNM give the same performance with respect to the temporal correlation properties. Fig. 9 and Fig. 10 show the CFs for the reference and simulation models using the LPNM and MLPNM. It was observed that the error function takes a maximum value $\max\{e_T(\delta_T,\tau)\} = 0.09$ for the LPNM, whereas the maximum error value is $\max\{e_T(\delta_T,\tau)\} = 0.1$ for the MLPNM. However, it was noticed that the error function decreases for the MLPNM.

V. CONCLUSION

In this paper, the methods used for modelling the MIMO M2M channels of the two-ring model are studied for both isotropic- and non-isotropic scattering cases. In this context, three new methods are suggested to design the simulation model of the MIMO channel: MEMEDS, NMMEA and MLPNM. The performance of each proposed method was compared with the original method by comparing the statistical properties of the reference and simulation models, where the results showed the superiority of the proposed methods in improving the performance of the temporal and spatial correlation characteristics of the simulation model, thus it can be said that this research can help in improving performance of the statistical properties of the simulation model by developing the methods used in the MIMO channel modelling. Finally, a more accurate and efficient MIMO M2M simulation model was obtained.

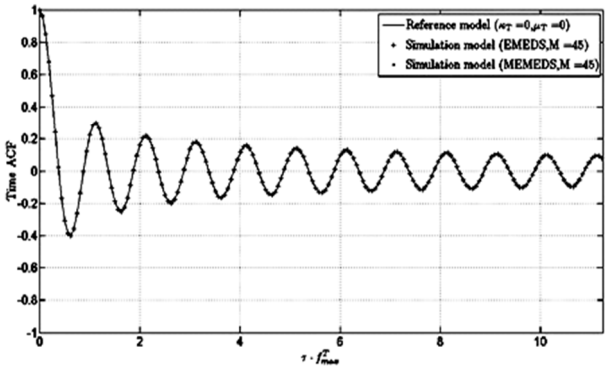

Fig. 2. ACFs comparison of the reference and simulation models using EMEDS and MEMEDS, in the case of isotropic scattering
$(\kappa_T = 0, \mu_T = 0^\circ, M = 45)$

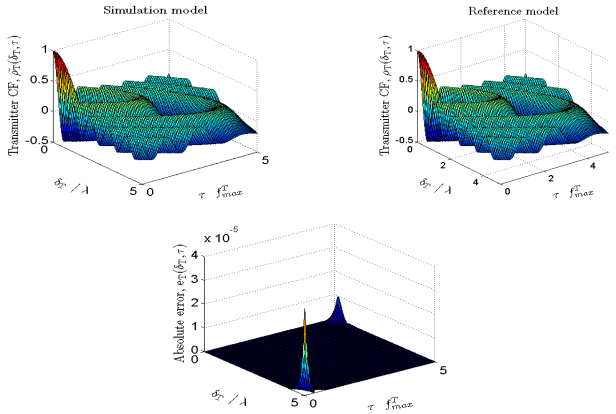

Fig. 3. CFs comparison of the reference and simulation models using EMEDS in the case of isotropic scattering
$(M = 45, \kappa_T = 0, \mu_T = 0^\circ, \beta_T = 90^\circ, \alpha_v^T = 60^\circ)$

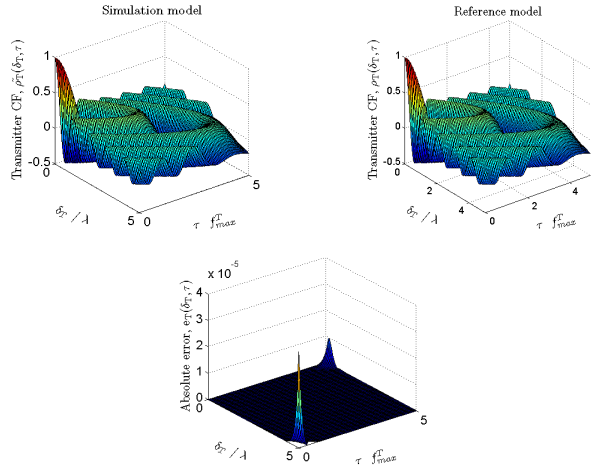

Fig. 4. CFs comparison of the reference and simulation models using MEMEDS in the case of isotropic scattering
$(M = 45, \kappa_T = 0, \mu_T = 0^\circ, \beta_T = 90^\circ, \alpha_v^T = 60^\circ)$

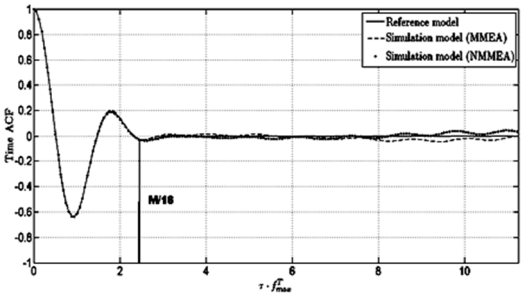

Fig. 5. ACFs comparison of the reference and simulation models using MMEA and NMMEA in the case of non-isotropic scattering
$(\kappa_T = 30, \mu_T = 60^\circ, M = 45)$

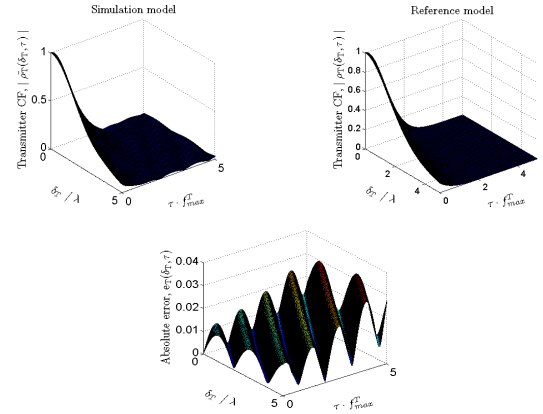

Fig. 6. CFs comparison of the reference and simulation models using MMEA in the case of non-isotropic scattering
$(M = 45, \kappa_T = 30, \mu_T = 60^\circ, \beta_T = 90^\circ, \alpha_v^T = 0^\circ)$

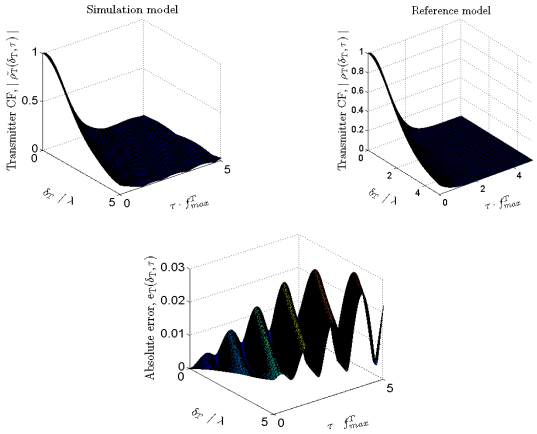

Fig. 7. CFs comparison of the reference and simulation models using NMMEA in the case of non- isotropic scattering

$(M = 45, \kappa_T = 30, \mu_T = 60^\circ, \beta_T = 90^\circ, \alpha_v^T = 0^\circ)$

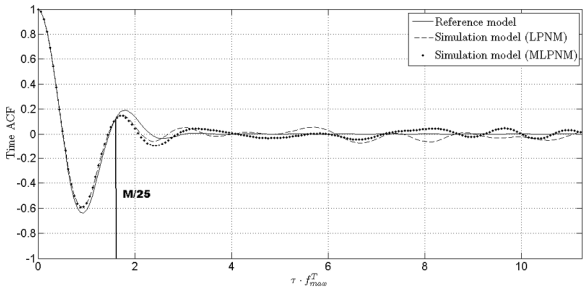

Fig. 8. ACFs comparison of the reference- and simulation models using LPNM and MLPNM in the case of non-isotropic scattering

$(\kappa_T = 30, \mu_T = 60^\circ, M = 45)$

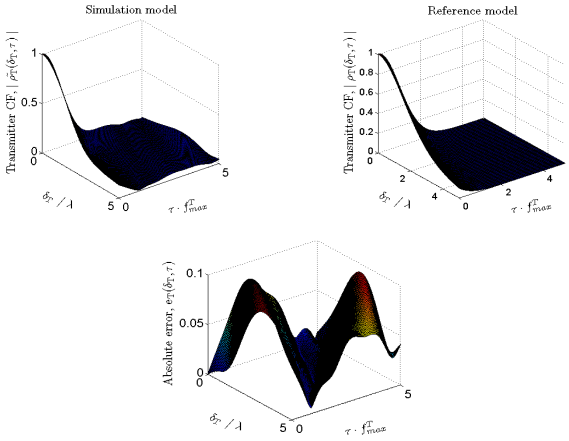

Fig. 9. CFs comparison of the reference and simulation models using LPNM in the case of non-isotropic scattering

$(M = 45, \kappa_T = 30, \mu_T = 60^\circ, \beta_T = 90^\circ, \alpha_v^T = 0^\circ)$

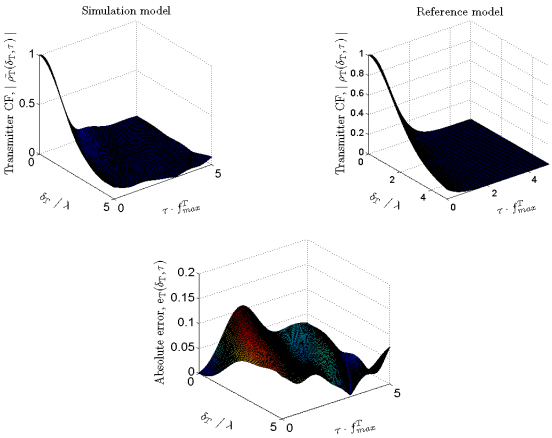

Fig. 10. CFs comparison of the reference and simulation models using MLPNM in the case of non-isotropic scattering

$(M = 45, \kappa_T = 30, \mu_T = 60^\circ, \beta_T = 90^\circ, \alpha_v^T = 0^\circ)$

REFERENCES

[1] R. Wang and D. Cox, "Channel modeling for ad hoc mobile wireless networks," *Proc. IEEE VTC'02-Spring*, Birmingham, USA, May 2002, pp. 21–25.

[2] IEEE P802.11p/D2.01, "Standard for wireless local area networks providing wireless communications while in vehicular environment," Tech. Rep., Mar. 2007.

[3] M. Pätzold, *Mobile Radio Channels*, 2nd ed, John Wiley & Sons, 2012.

[4] M. Shih, K. D. Huang, C. Yeh and H. Wei, "To wait or to pay: a game theoretic mechanism for low-cost M2M and mission-critical M2M," *IEEE Transactions on Wireless Communications*, vol. 15, no. 11, pp. 7314-7328, November 2016.

[5] A.S. Akki and F. Haber, "A statistical model for mobile-to-mobile land communication channel, " *IEEE Trans. on Veh. Tech.*, vol. 35, pp. 2–10, Feb. 1986.

[6] O Alzoubi, "Improving the Performance of MIMO Fading Channel Simulators Using New Parameterization Method," *Journal of Engineering Sciences and Information Technology*, vol. 4, pp. 61-76.

[7] A. S. Akki, "Statistical properties of mobile-to-mobile land communication channels," *IEEE Trans. on Veh. Technology*, vol. 43, pp. 826–831, Nov. 1994.

[8] M. Pätzold, B. O. Hogstad, N. Youssef, and D. Kim, "A MIMO mobile-to-mobile channel model: Part I-the reference model," *Proc. IEEE PIMRC 05*, Berlin, Germany, Sep. 2005.

[9] A. G. Zajic and G. L. Stüber, "Space-time correlated mobile-to-mobile channels: modelling and simulation," *IEEE Trans. Veh. Technol.*, vol. 57, no. 2, pp. 715–726, Mar. 2008.

[10] X. Cheng, C.-X. Wang, D. I. Laurenson, S. Salous, and A. V. Vasilakos, "An adaptive geometry-based stochastic model for non-isotropic MIMO mobile-to-mobile channels," *IEEE Trans. Wireless Commun.*, vol. 8, no. 9, pp. 4824–4835, Sept. 2009.

[11] X. Cheng, C.-X. Wang, and D. I. Laurenson, "A geometry-based stochastic model for wideband MIMO mobile-to-mobile channels," *Proc. IEEE GLOBECOM'09*, Hawaii, USA, Nov.–Dec. 2009.

[12] C.-X. Wang, X. Cheng, and D. I. Laurenson, "Vehicle-to-vehicle channel modeling and measurements: recent advances and future challenges," *IEEE Commun. Mag.*, vol. 47, no. 11, pp. 96–103, Nov. 2009.

[13] A. Abdi, J. A. Barger, and M. Kaveh, "A parametric model for the distribution of the angle of arrival and the associated correlation function and power spectrum at the mobile station," *IEEE Trans. Veh. Technol.*, vol. 51, no. 3, pp. 425–434, May 2002.

[14] B. O. Hogstad, M. Pätzold, N. Youssef, and D. Kim, "A MIMO mobile-to-mobile channel model: part II—the simulation model," *in Proceedings of the 16th International Symposium on Personal, Indoor and Mobile Radio Communications (PIMRC '05)*, pp. 562–567, Berlin, Germany, September 2005.

[15] M. Pätzold, U. Killat, F. Laue, and Y. Li, "On the statistical properties of deterministic simulation models for mobile fading channels," *IEEE Transactions on Vehicular Technology*, vol. 47, no. 1, pp. 254–269, 1998.

[16] C. A. Gutierrez-Diaz-De-Leon and M. Pätzold, "Sum-of- sinusoids-based simulation of flat fading wireless propagation channels under non-isotropic scattering conditions," in *Proceedings of the 50th Annual IEEE Global Telecommunications Conference (GLOBECOM '07)*, pp. 3842–3846, Washington, DC, USA, November 2007.

[17] C. A. Gutierrez-Diaz-De-Leon and M. Pätzold, "*Efficient sum of-sinusoids-based* simulation of mobile fading channels with asymmetrical Doppler power spectra," in *Proceedings of the 4th IEEE International Symposium on Wireless Communication Systems (ISWCS '07)*, pp. 246–251, Trondheim, Norway, October 2007.

[18] M. Pätzold, U. Killat, and F. Laue, "A deterministic digital simulation model for Suzuki processes with application to a shadowed Rayleigh land mobile radio channel," *IEEE Trans. Veh. Technol.*, vol. 45, no. 2, pp. 318–331, May 1996.

[19] O. Alzoubi and M. Wainakh, "Improving the Performance of Fading Channel Simulators Using New Parameterization Method," *International Journal of Electronics and Electrical Engineering (IJEEE)*, Vol. 4, No. 5, 443-448 October 2016. www.ijeee.net. published by Int. J. Electron. Electr. Eng.